

Numerical Simulation of Wind Loading on Ground-Mounted East-West Solar Farms

James Horsley¹, Victor Rego² and Con Doolan¹

¹*School of Mechanical and Manufacturing Engineering, UNSW, Sydney, Australia*

²*5B Solar, Sydney, Australia*

The structural design of solar photovoltaic (PV) racking systems is driven predominantly by wind loading. Misunderstanding of the wind loading on a system can drive up the cost of a solar farm either through overengineering and unnecessary material costs, or through lack of structural integrity and subsequent failure of the system in high winds. Previous studies have examined wind loads exerted on fixed-tilt and single-axis tracker racking systems however little has been discussed on other types of racking systems.

In this study, Reynolds-Averaged Navier-Stokes simulations were conducted to examine the wind flow field around, and wind loads exerted on, a high ground coverage, east-west solar PV array. Simulations focused on 5B's MAVERICK (MAV) array, shown in Figure 1, however variations on the system was also simulated and a comparison was made to fixed-tilt arrays. The numerical simulation was validated by the pressure distribution over the fixed-tilt array compared against the experimental results of Abiola-Ogendengbe (2015) on the same array. The pressure coefficients of the numerical simulation on the full-scale MAV (5.5m (W), 36.7m (L), 2.3m (H)) was also compared with wind tunnel data on a 1:20 scale model.



Figure 1. 5B's east-west MAVERICK array

It was found that the presence of a clearance between the MAV and the ground drastically increased the load experienced by the array when wind approached from the east or west (i.e. normal to the ridge line). As shown by the area-averaged pressure coefficients on each panel in Figure 2 (a), the average load on the modules was observed to increase from no clearance to a 250mm clearance however decrease from 250mm to 500mm. It is clearly seen in the pressure coefficient distribution on the upper surface of the panels in Figure 2 (b) that the different ground clearances had little effect on the flow over the upper surface of the panels. This indicates the discrepancies were predominantly due to wind flow underneath the array. The drop in pressure from 250mm to 500mm was due to the clearance of flow blockage under the beams with the higher ground clearance. In the 250mm ground clearance, the blunt body of the beam created a higher pressure on the upwind side of the beam. This led to the short flow separation and recirculation seen by the streamlines in Figure 2 (c) downwind of each beam. In contrast, the streamlines in Figure 2 (d) of the 500mm ground clearance show a smoother flow under the MAV as the higher ground clearance reduces the effect of the beam on the pressure.

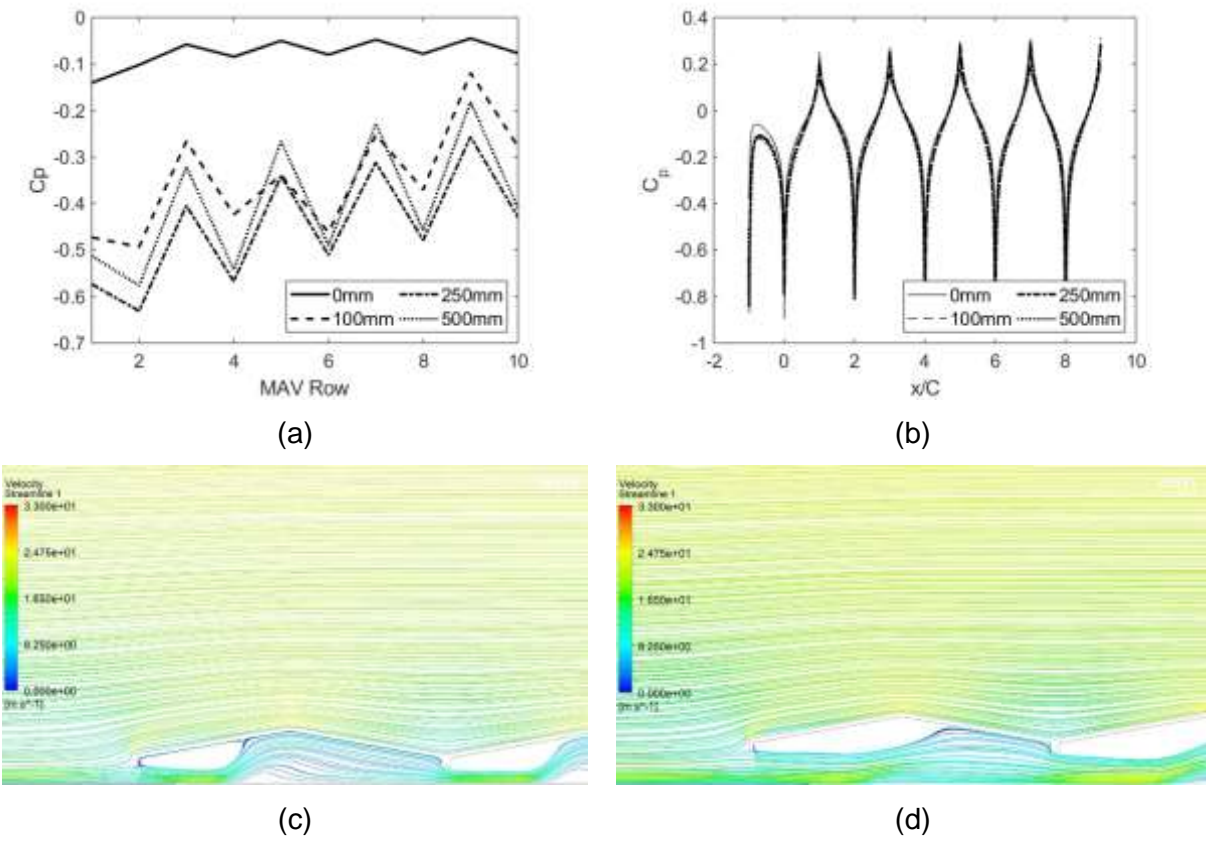


Figure 2. The effect of ground clearance. (a) shows the average pressure coefficient across each panel; (b) shows the pressure coefficient distribution on the upper surface of the panels; (c) and (d) show the streamlines around the MAV with a 250mm and 500mm ground clearance respectively

The effect of row positioning was also investigated. Figure 3 (a) indicates the largest difference on the upper surface of the panels was observed between the first and second waves (pairs of east and west panels) of the MAV. The sharp angle of inclination between the beam and the first panel creates a flow separation that generates a low pressure zone at the leading edge of the panel. The drop in net pressure coefficient between the second and fifth waves (Figure 3 (c)) was again driven by the drop in pressure on the lower surface of the panels (Figure 3 (b)). This energy loss was due in part to the frictional effects of the fluid flowing over the panels and the ground. The primary cause of the energy loss however was likely the flow separation and turbulent flow caused by the beams. The pressure loss over the MAV was observed to be lower when the beams were removed from the model.

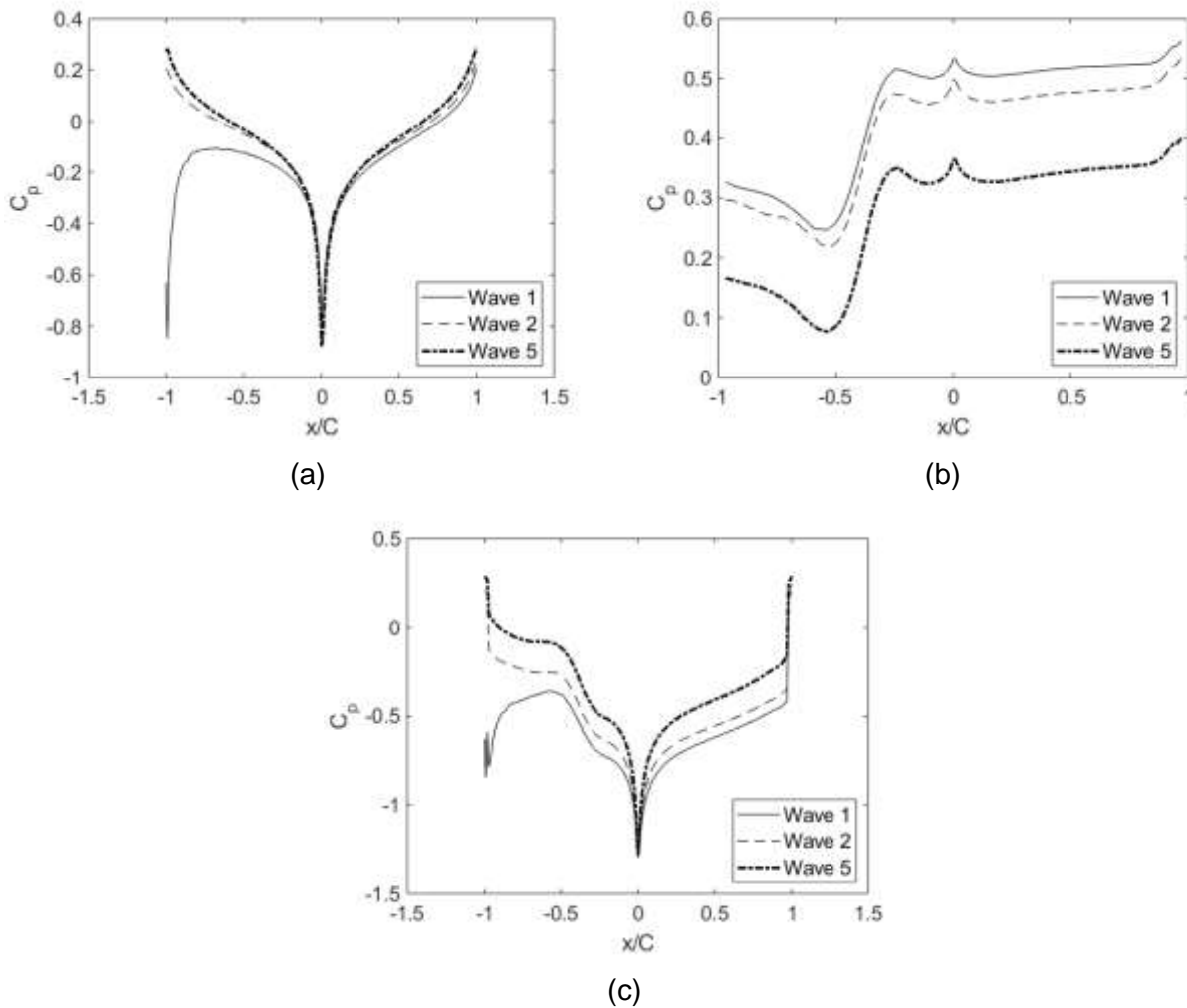


Figure 3. The effect of row positioning on the pressure coefficient distribution on the (a) upper, (b) lower and (c) net surfaces of the panels with a 250mm ground clearance

The pressure distribution on different racking systems can be compared in Figure 4. A variation on the traditional design of the MAV was modelled by removing the concrete beams. Without the beams, the flow separation on the lower surface of the panels was reduced which resulted in a higher velocity flow. The increase in flow velocity corresponded with a lower pressure region below the MAV and hence lower net uplift on the MAV. The distribution on the fixed-tilt systems was profoundly different to that on the east-west systems. The sharp angles of inclination on the windward and leeward edge created a large recirculation region and hence low pressure region behind the panel. This increased the downward net pressure on the panel. The magnitude of the peak pressure was larger on the fixed-tilt structures than the east-west.

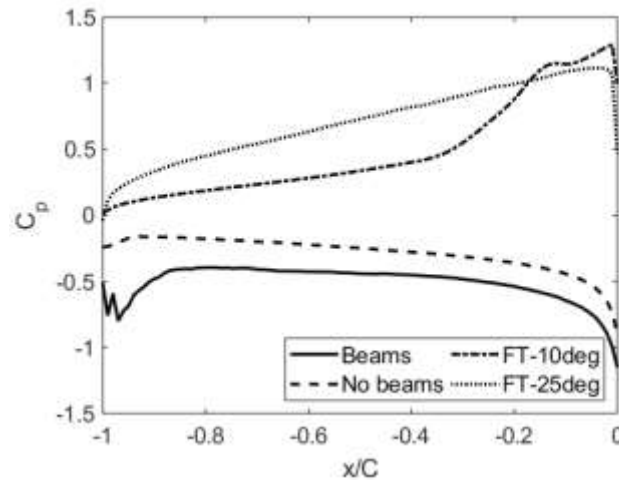


Figure 4. The pressure coefficient distribution on the first row of east-west arrays with a 500mm ground clearance compared to fixed-tilt arrays at 10° and 25° pitches

This study will also examine the effect of wind direction on the wind load experienced by the MAV. 3D simulations will be conducted with incoming wind at 0°, 30°, 45° and 90° from normal to the ridge line. The observations from this study could be used to improve the design of racking systems for east-west solar arrays by focusing structural reinforcement on areas of need and providing insights for the design of load reduction mechanisms such as wind barriers. The consequence of this is the potential to reduce racking system costs and improve the cost competitiveness of solar PV arrays with other power generation systems.

References

Abiola-Ogedengbe, A., Hangan, H. and Siddiqui, K., 2015, 'Experimental investigation of wind effects on a standalone photovoltaic (PV) module', *Renewable Energy*, 78, p657-665.